



Climate Sensitivity Parameter in the Test of the Mount Pinatubo Eruption

Antero Ollila^{1*}

¹Department of Civil and Environmental Engineering (Emer.), School of Engineering, Aalto University, Otakaari 1, Box 11000, 00076 AALTO, Espoo, Finland.

Author's contribution

The sole author designed, analyzed and interpreted and prepared the manuscript.

Article Information

DOI: 10.9734/PSIJ/2016/23242

Editor(s):

- (1) Yichi Zhang, Key Laboratory of Water Cycle & Related Land Surface Processes, Institute of Geographic Sciences and Natural Resources Research, Chinese Academy of Sciences, China.
- (2) Ismail Gultepe, Environment Canada, Cloud Physics and Severe Weather Res. Section, Canada.
- (3) Abbas Mohammed, Blekinge Institute of Technology, Sweden.

Reviewers:

- (1) Anonymous, University of St. Thomas, USA.
 - (2) Mahmut Dogru, Bitlis Eren University, Turkey.
 - (3) S. B. Ota, Institute of Physics, Bhubaneswar, India.
 - (4) Bharat Raj Singh, Technical Campus, Lucknow, India.
- Complete Peer review History: <http://sciencedomain.org/review-history/13553>

Original Research Article

Received 21st November 2015
Accepted 14th February 2016
Published 4th March 2016

ABSTRACT

The author has developed a dynamic model (DM) to simulate the surface temperature change (ΔT) caused by the eruption of Mount Pinatubo. The main objectives have been 1) to test the climate sensitivity parameter (λ) values of $0.27 \text{ K}/(\text{Wm}^{-2})$ and $0.5 \text{ K}/(\text{Wm}^{-2})$, 2) to test the time constants of a simple first-order dynamic model, and 3) to estimate and to test the downward longwave radiation anomaly (ΔLWDN). The simulations show that the calculated ΔT of DM follows very accurately the real temperature change rate. This confirms that theoretically calculated time constants of earlier studies for the ocean (2.74 months) and for the land (1.04 months) are accurate and applicable in the dynamic analyses. The DM-predicted ΔT values are close to the measured value, if the λ -value of $0.27 \text{ K}/(\text{Wm}^{-2})$ has been applied but the λ -value of $0.5 \text{ K}/(\text{Wm}^{-2})$ gives ΔT values, which are about 100% too large. The main uncertainty in the Mount Pinatubo analyses is the ΔLWDN flux, because there are no direct measurements available during the eruption. The author has used the measured ERBS fluxes and has also estimated ΔLWDN flux using the apparent transmission measurements. This estimate gives the best and most consistent results in the simulation. A simple analysis shows that two earlier simulations utilising General Circulation Models (GCM) by two research groups are depending on the flux value choices as well as the measured ΔT choices. If the commonly used minimum value of -6 Wm^{-2} would have been used for the shortwave anomaly in the GCM

*Corresponding author: E-mail: aveollila@yahoo.com;

simulations, instead of -4 Wm^{-2} , the ΔT values would differ from the measured ΔT values almost 100%. The main reason for this error seems to be the λ -value of $0.5 \text{ K}/(\text{Wm}^{-2})$.

Keywords: Global warming; climate sensitivity parameter; climate response time; radiative forcing response; downward radiative fluxes; Mount Pinatubo eruption.

1. INTRODUCTION

1.1 Objectives and Symbols

The Mount Pinatubo eruption in 1991 caused a global cooling during the next five years as the incoming shortwave radiation was reduced by 6 W/m^2 offering a unique opportunity to test and to analyse the various phenomenon of the climate system. Water vapour feedback has remained a topic of debate since 1990 and the eruption can be used to analyse this effect also. The first objective of this paper is to test the two climate sensitivity parameter values which have been commonly used in the scientific studies. The second objective is to test the climate system time constants describing the dynamic behaviour of the climate exposed to a relative big and sudden change. The third objective is to estimate and to test the downward longwave radiation anomaly (ΔLWDN). In the simulations a theoretical feedback property of the climate system has been also tested.

Table 1 includes all the symbols, abbreviations, acronyms and definitions used repeatedly in this paper.

1.2 The Mount Pinatubo Eruption

The main eruption of the Mount Pinatubo volcano (15.1°N , 120.3°E) on the island of Luzon in the Philippines began on the 3rd of June, 1991 and concluded on the next day. Four large explosions generated eruption columns reaching the heights of up to 24 km in the stratosphere. The estimate of the stratospheric mass increase was 14–20 Mt of SO_2 , which created 21–40 Mt of $\text{H}_2\text{SO}_4\text{-H}_2\text{O}$ aerosols [1]. The eruption also injected vast quantities of minerals and metals into the troposphere and stratosphere in the form of ash particles. The aerosols formed a global layer of sulfuric acid haze over the globe and the global temperatures dropped about 0.5°C in the years 1991 – 1993.

The sulphate aerosols caused scattering of the visible light and therefore the incoming radiation scattered more effectively back into space. Thus the albedo of the Earth increased leading to a

cooling at the Earth's surface. On the other hand the plants utilized the climate conditions, because they could photosynthesize more effectively in the diffuse sunlight [2,3]. As a result of the more intensive photosynthesis, there was a negative anomaly of the global CO_2 concentration increase rate.

Table 1. List of symbols, abbreviations, and acronyms

Acronym	Definition
DM	One dimensional dynamic model
AT	Apparent transmission
ENSO	El Niño Southern Oscillation
ERBS	NASA's Earth Radiation Budget Satellite
GCM	General Circulation Model
ISCCP	International Satellite Cloud Climatology Project
LW	Longwave
LWDN	LW radiation flux downward
LWUP	LW radiation flux upward
LWSRF	LW radiation emitted by the surface
OLR	Outgoing longwave radiation
ONI	Oceanic Niño Index
RF	Radiative forcing change
SW	Shortwave
SWATM	SW radiation flux absorbed by the atmosphere
SWIN	SW radiation flux incoming at the TOA
SWSRF	SW radiation flux incoming at the surface
TOA	Top of the atmosphere
TPW	Total precipitable water
T	Surface temperature
Tm	1DM-predicted surface temperature change
Tav	Average surface temperature change by four datasets
Tmsu	Surface temperature change by UAH MSU dataset
Tav-e	Tav with ENSO correction
Tmsu-e	Tmsu with ENSO correction
TCS	Transient climate sensitivity
λ	Climate sensitivity parameter
Δ	Anomaly or change

Subscript_n means step n in time domain.

Because the eruption happened at one point, it took several weeks before the global effect was fully developed. The volcanic aerosol cloud encircled the Earth in 21 days driven by the easterly winds in the tropical stratosphere. It covered about 42% of the Earth in two weeks [4]. In Fig. 1 are depicted the global temperature [5] and the apparent transmission measured at Mauna Loa [6] (19.3°N, 155.4°W). It can be seen that there is delay between the temperature response and the apparent transmission (AT) describing the reduction of the incoming shortwave (SW) radiation.'

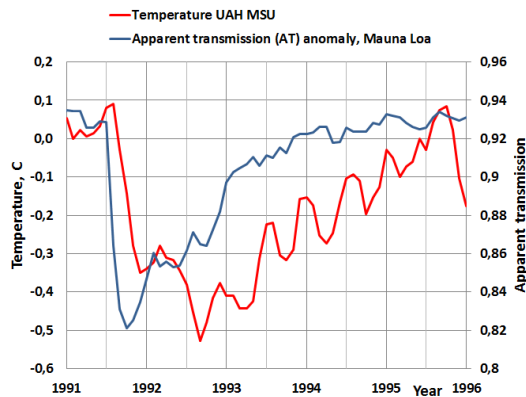


Fig. 1. The global satellite temperature and the apparent transmission measured at Mauna Loa, Hawaii

In Fig. 2 the apparent transmissions (AT) are depicted at the various sites on the northern hemisphere [7]. It can be seen that the absolute values of the AT values are different depending mainly on the local conditions. For example, the low values of the Japanese sites describe the air quality of the local conditions. The large value of the Mauna Loa is due to the fact that it is at the altitude of 3.4 km in the middle of the Pacific. An important feature thinking the analysis methods of this study is that the percentage decreases are very close to each other in the range from 10.1% to 13.2%.

The sites in Fig. 2 cover almost 85% of the northern hemisphere. Thomas [8] has analyzed the global apparent transmission measurements after the eruption. The analysis shows that the aerosol cloud was covering the latitudes from 60S to 60N after three months and practically uniform over the hemispheres after six months. This is also the moment of the maximum temperature decrease. The main role in spreading the cloud had planetary scale waves in high latitudes, which transported the volcanic

aerosol from the tropics to high latitudes. The reason why the decrease of apparent transmission value was almost the same at the high latitudes as in the tropics is probably due to the zenith angle. Even though the sulphate cloud would be thinner at the high latitudes, the sunlight has a longer pathway through the atmosphere. This phenomenon can compensate the effects of possible thinner cloud conditions.

Two conclusions can be drawn from these figures. The global delay called a dead time in process dynamics, is estimated to be 1.6 months between the incoming SW radiation change and the global surface temperature response. This value is used in the dynamical analyses of this study.

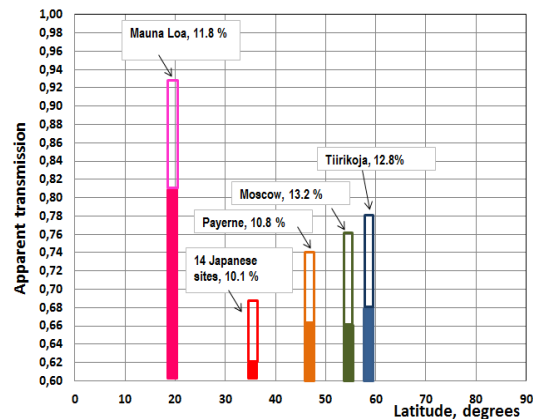


Fig. 2. The apparent transmission values at the various sites. The percentage values show the maximum decreases of the apparent transmissions after the eruption and they are represented by light bars inside the normal apparent values (total bar length)

Another conclusion is that after the fully developed coverage of the sulphate cloud in the stratosphere, the radiation effect changes can be estimated to happen simultaneously over the globe. Therefore it is justified to use the one dimensional (1D) approach in developing a dynamic model (called DM) for analysing the temperature versus radiation flux relationships.

1.3 Literature Study

There have been numerous Pinatubo studies on the three major fields. The first is on the aerosol and chemical effects of the Pinatubo particles. The second is focused on optical properties of the aerosol particles and on the radiative forcing. The third is on the responses to the forcing

affecting the temperature and the circulation patterns.

This paper concentrates on the dynamic behaviour of the surface temperature changes caused by the radiative flux changes. Therefore the survey of the earlier studies covers only the subjects which are relevant for this study.

Even though the Pinatubo eruption is the best documented major eruption so far, there was an essential radiative flux, which was not directly measured during the eruption. This was the LW downward radiation flux (LWDN), which is essential, because it compensates the major portion of the cooling effects of the reduced SW downward radiation flux (SWIN) decrease during the early phases of the eruption [9].

The World Climate Research Programme (WCRP) Radiative Fluxes Working Group initiated a new Baseline Surface Radiation Network (BSRN) to support the research projects. Some years later the BSRN was incorporated into the WCRP Global Energy and Water Cycle Experiment (GEWEX). The BSRN network stations started to operate in 1992 and that is why these valuable measurements were not available during the Pinatubo eruption.

There has been a special GEWEX project to assess the surface radiation budget datasets [10] based on the available data at the top of the atmosphere (TOA). By studying the GEWEX results, the author's conclusion is that the LWDN fluxes could not be estimated reliably in this project based on the other existing flux data. Therefore a major challenge in this study is to estimate the Δ LWDN flux trend during the Pinatubo eruption.

In Fig. 3 the main radiative fluxes of the Earth are illustrated [11,12]. The climate forcing effect of a volcano eruption can be analysed in the same way as the cloud change forcing. Normally the cloud forcing has been calculated as the sum of changes in the downward SW flux change and outgoing LW flux change between the clear and all-sky conditions. Applying this same method, the radiative forcing (RF) caused by the eruption, is the sum of Δ SWIN and Δ LWUP and it is called aerosol radiative forcing [13]. The change in the flux values is calculated between the normal conditions and during or after the eruption. Because the outgoing LW flux is reduced during the early phases of the eruption, it is a sign that there is cooling happening on the surface.

The RF value calculated in this way is normally called radiative or climate forcing (RF). Actually it is only a measure of the real RF. There are two fluxes which have the real forcing effect on the Earth's surface temperature (T) and they are SWIN and LWDN. They are the only fluxes, which form the radiation input on the surface. In the change from the all-sky to the cloudy sky conditions, the change of LWUP at the TOA is -11 Wm^{-2} and the change of LWDN at the surface is $+14.3 \text{ Wm}^{-2}$ [12]. These flux values show that if the clear sky conditions do not prevail, the LWUP change is not equal to the real warming/cooling impact on the surface caused by the LWDN flux change. This example also shows that the LWDN flux change is greater than the LWUP flux change. The major reason for this difference is that the cloudy sky values are actually measured in the dynamic situation and the LWUP flux is not in the real equilibrium value.

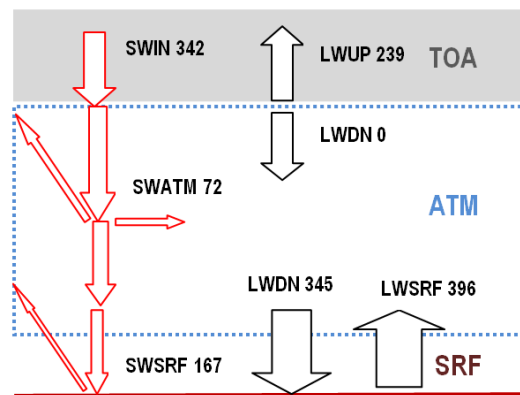


Fig. 3. The main radiative fluxes of the Earth's energy balance

The small particle sizes less than $1 \mu\text{m}$ are more effective in reflecting the SW solar radiation SWIN than they are at reflecting the LW radiation emitted by the surface. According to a comprehensive study [1], the smallest particles were sulphuric acid/water droplets and the largest particles were ash fragments. The cooling and warming effects of the aerosols and particles depend on the particle sizes. The LWDN flux increases especially during the early phases of the eruption because there are larger aerosol particles more in the atmosphere than in the later phases. Therefore the warming effect of LWDN is the most effective at the same time as the cooling is in maximum [1,9]. The stratospheric ash layer settled down just above the troposphere staying there until March 1992. The particle size measurements [1,4] showed that

there was a peak in both small and large particle sizes after a few months after the eruption but by 1993 the high measurements values were decaying back to pre-eruption values.

The ash cloud in the high altitudes of the atmosphere absorbs and emits radiation. This ash cloud had a measureable warming effect on the northern hemisphere winter temperatures [14,15]. The ash cloud has about the same effect as the clouds have in the cold climate conditions, it will prevent the cooling of the surface. In this way it has a net warming effect.

The radiative forcing (RF) at TOA has a linear relationship to the global mean surface temperature change ΔT , if the equilibrium state is assumed [16]:

$$\Delta T = \lambda RF, \quad (1)$$

where λ is the climate sensitivity parameter, which is a nearly invariant parameter having a value of $0.5 \text{ K}/(\text{Wm}^{-2})$. IPCC uses still equation (1) in its latest report AR5 but IPCC no longer keeps the value of λ almost constant [17]. A general experience and also a common practice is to approximate the small changes around the operating point to be linear by nature. The most probable change of RF by the end of this century is 6 Wm^{-2} according to RCP6 (Representative Concentration Pathways) [17]. This change is only 2.5% about the average value of OLR (outgoing longwave radiation) value of 239 Wm^{-2} .

The author carried out a study about this issue utilizing the MODTRAN code [18]. The concentration of CO_2 varied from 357 ppm to 700 ppm and the sky conditions were clear and cloudy, which were combined to calculate the all-sky values. The average global atmosphere profiles for GH gases, temperature and pressure were applied. The results show that the maximum nonlinearity between the OLR fluxes was 0.01% and the maximum variation in λ values was 2.5%, when the surface temperature varied $\pm 1^\circ\text{C}$. These results show that the equation (1) is applicable for small RF and temperature changes.

Ollila has analysed [19] the future warming values based on the RF values of greenhouse gases. This analysis showed that the warming values of RCP2.5, RCP4.5, and RCP6 could be calculated using the λ value of $\sim 0.37 \text{ K}/(\text{Wm}^{-2})$. IPCC has calculated RCP warming values applying GCMs but they do not inform the

possible λ values. On the other hand IPCC reports in AR5 [17] that the transient climate sensitivity (TCS) value is likely to lie in the range 1 to 2.5°C giving the average value 1.75°C . This value is almost the same as calculated by equation (1): $\Delta T = 0.5 \text{ K}/(\text{Wm}^{-2}) * 3.7 \text{ Wm}^{-2} = 1.85 \text{ K}$. The conclusion is that IPCC is very inconsistent in using λ values and equation (1). If λ is not “nearly invariant parameter”, IPCC should have introduced something more credible scientific evidence about the real nature of λ .

This inconsistency may be linked to the warming values of the recent RF values. There should not be any of IPCC’s own climate models, but in reality there is such a model called “Radiative Forcing by Emissions and Drivers” which has a summary leading to the value of 2.34 Wm^{-2} according to AR5 [17]. IPCC denies that there is any IPCC’s model but the fact is that the IPCC organization has selected a number of research studies, which have been used in creating their presentation. There are private researchers who do not make the same selections and therefore their models are different. If equation (1) is applied in the same way as calculating the TCS value above, the warming value of 2.34 Wm^{-2} would be 1.17°C in 2011. IPCC does not show this temperature increase in the AR5 [17], and one reason might be that it is 38% greater than the observed value of 0.85°C .

The possible water feedback is the only essential feedback in TCS calculations. In the referred GCM studies applied in the Pinatubo analyses, there are no reported λ values. The lambda value of $0.5 \text{ K}/(\text{Wm}^{-2})$ means that there is a positive water feedback included into a model. The assumption that there is a positive water feedback in the climate models means that relative humidity (RH) should be constant despite the moderate warming/cooling of the atmosphere. This property of the positive water feedback would double the warming effects of GH gases according to AR4 [16]. IPCC reports in AR5 that the positive water feedback can amplify any forcing by a typical factor between two and three [17]. This means that understanding of water feedback magnitude is not becoming more accurate but it has become more inaccurate.

The issue of a constant RH can be studied by simply looking at the RH trends since 1948, which are depicted in Fig. 4 [20]. It is clear that RH has varied quite a lot. Even though the early RH measurements may be unreliable, the measurements since 1980 have better

technology and they are very accurate and reliable.

The positive water feedback and high climate sensitivity (CS) of climate models is a well-known feature. Normally the equilibrium CS varies from 1.5°C to 4.5°C [21], which means that the variation of TCS (Transient climate sensitivity) is about half of this range. However there are several studies, which have calculated the climate sensitivity value to be about 1.0 – 1.2°C [22-25] using the same radiative forcing value of 3.7 Wm⁻² for CO₂ as IPCC uses. It means a lower λ value of about 0.27 - 0.3 K/(Wm⁻²). Some researchers have calculated even lower values like ~0.6°C for climate sensitivity [19,26] or 0.7°C [27]. Ollila [19] has calculated the λ value using three different methods and his results vary between 0.245 and 0.331 the most reliable value being 0.268 K/(Wm⁻²). In this study these two most common values have been applied: 0.27 K/(Wm⁻²) and 0.5 K/(Wm⁻²).

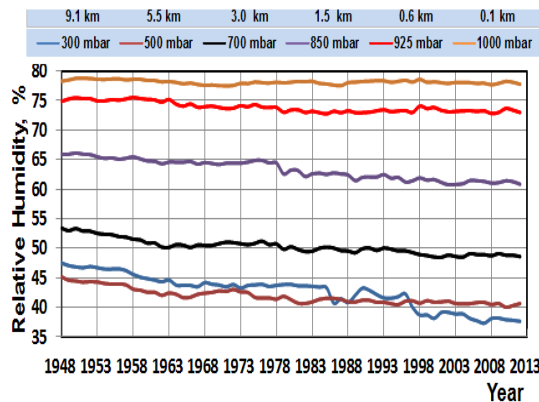


Fig. 4. The global relative humidity trends according to NOAA at different altitudes in the troposphere

The forcing studies can be classified into two categories namely forcing calculations utilising General Circulation Models (GCM) 1) for simulations of spatial flux and temperature changes [8,28-31,2] other simulations resulting the surface temperature change. In respect to this study only the latter studies are relevant.

One of the earliest studies was that of Hansen et al. [32]. They used the GISS global climate model to assess the preliminary impacts of the Pinatubo eruption. In their calculations they used the peak value of -4 Wm⁻² for ΔSWIN and they could show that the simulated ΔT was about -0.5 °C. The most common value of ΔSWIN has been -6 Wm⁻² [8,13,14,29,33]. This value is also used in this study.

In the later study Hansen et al. [34] applied the same peak value of -4 Wm⁻² in the GCM simulations by name SI94 and GRL92. Soden et al. [35] applied a GCM and as input data they used ERBS fluxes in calculating the RF values. They also included the absolute atmospheric water content as a variable. The peak value of -4 Wm⁻² was used for ΔSWIN. Their major result was the GCM simulations could calculate the ΔTm values close to the measured value, if the positive water feedback was included. The water content was calculated using the NASA Water Vapor Project (NVAP) values [36].

In Fig. 5 the NVAP dataset values as well the NCEP/NCAR (National Center for Environmental Prediction / National Center for Atmospheric Research) values are depicted [37]. The NVAP water content trends show great seasonal changes of about 3 TPW mm. Soden et al. [35] have reported that there has been ~0.75 TPW mm peak reduction during the Pinatubo eruption. The graphs show that the peak reduction estimate [23] can be regarded a correct estimate. This choice of using the peak values only can be questioned, because the trend line of NVAP-M values show increased rate of absolute water content. A justified procedure would be to use the monthly values but then the water feedback effects would be huge. Because the seasonal water content variations depend mainly on the northern hemisphere seasonal changes, a better method might be to combine zonal temperature and water content values.

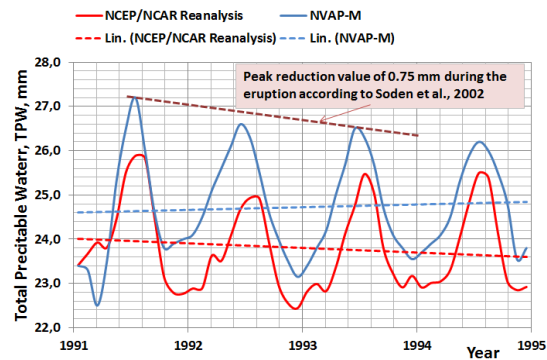


Fig. 5. The graphs of water contents according to NVAP-M and NCEP/NCAR datasets

In Fig. 5 it can be noticed that there are opposite trends in these datasets during the Pinatubo eruption. It is quite impossible to know, which of these datasets is correct and therefore the question of positive or negative water feedback

cannot be reliably tested utilising the Pinatubo case and the global water content trends.

2. RADIATIVE FLUXES AND FORCING ANOMALIES CAUSED BY THE ERUPTION

The two SWIN flux datasets available during the eruption are ISCCP [38] and ERBS [39]. They are depicted in Fig. 6. Both datasets are unstable and spiky. The SWIN flux anomaly can also be estimated using the apparent transmission (AT) signal or optical depth measurements. In this case the AT signal of Mauna Loa has been used. The Δ SWIN flux anomaly has been assumed to follow exactly the trend of the AT-signal. The time of the minimum value of the AT-signal has been used to be also the time of the minimum value of the SWIN flux value of -6 Wm^{-2} . This estimate of Δ SWIN flux is depicted in Fig. 6 and it can be noticed that this flux is very stable and its trend follows very well the average form of ISCCP and ERBS fluxes. The smoothed Δ ERBS SWIN flux signal follows the estimated AT transformed Δ SWIN flux signal so well that they could be used between each other.

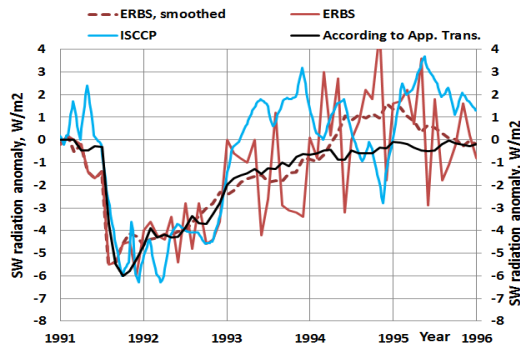


Fig. 6. SW downward radiation flux anomalies at TOA

Because there are no direct measurements of LWDN flux, it has been estimated. As realized before, the LWDN flux anomaly should follow the amount of large aerosol particle amounts in the atmosphere. Russell et al. [1] has a Fig. 6 in their paper containing optical depth measurements of the different particle size trends measured at Mauna Loa during the eruption.

It has been assumed that the smaller particle sizes from 0.382 to 0.500 μm are related to the Δ SWIN flux anomaly. The largest particle size is 1.020 μm and the graph of its aerosol optical depth has been used to estimate the Δ LWDN

flux. The peak values relationship between the 1.020 μm and 0.382/0.500 μm is 0.6. Using this relationship the peak value of estimated Δ LWDN flux anomaly would be $0.6 * (-6 \text{ Wm}^{-2}) = -3.6 \text{ Wm}^{-2}$. The Δ LWDN is been estimated to follow the aerosol optical depth signal of the particle size 1.020 μm at Mauna Loa and it is depicted in Fig. 7.

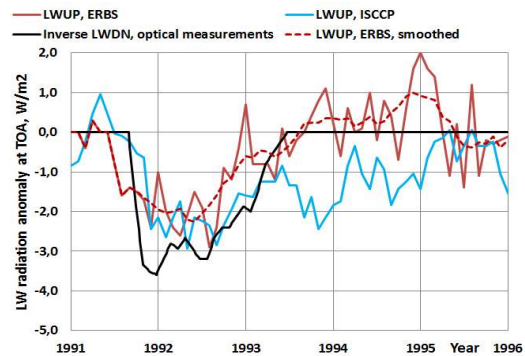


Fig. 7. LW radiation flux anomalies at TOA

In Fig. 7 it can be noticed that the peak value of estimated LWDN flux is greater than the Δ LWUP values measured at TOA by ISCCP and by ERBS. One explanation is that Δ LWUP fluxes depend mainly on the surface temperature and therefore there is a dynamic delay in comparison to the Δ LWDN flux. The full effect of this delay is about one year. In the dynamic situations like this Pinatubo eruption anomaly, the maximum temperature anomaly is about from 80% to 90% from the full effect. This difference is analyzed more deeply in the simulation section.

In the simulations the measured surface temperature anomaly ΔT is a reference. There are five dataset commonly available and four of them are depicted in Fig. 8 [5,40-42]. There are rather big differences in the trends. The difference between the HadCRT4 and the UAH MSU, which is a lower atmosphere temperature measured by satellites, is even 0.4°C around the beginning of the years 1992 and 1993. The UAH MSU trend has the largest minimum value during the eruption. Because of this situation, two surface temperature trends have been used as references namely Tmsu (UAH MSU dataset) and Tav (average of all four datasets).

Hansen et al. [34] and Soden et al. [35] have taken into account that the ENSO (El Niño Southern Oscillation) phenomenon had the maximum warming index in January 1992, when the Pinatubo eruption had the strongest cooling

effects. The researchers eliminated the ENSO effect by calculating a modified surface temperature of MSU UAH dataset. According to the graphs of these two papers, the ENSO corrected minimum peak of ΔT has been from -0.7°C to -0.75°C . They refer to the study of Santer et al. [43]. The author reads this same paper that the maximum mean volcanically induced cooling ΔT_{max} at the surface is from 0.35°C to -0.45°C and it is about double in the troposphere. ENSO certainly has a warming effect from 1991 to the end of 1992, and therefore this result is not logical, because the temperatures without ENSO corrections are about the same. There is a graph [43], where the temperature anomaly is about -0.75°C but it is for the troposphere and not for the surface. Another study of Thompson et al. [44] shows that the maximum warming effect of ENSO is only 0.14°C .

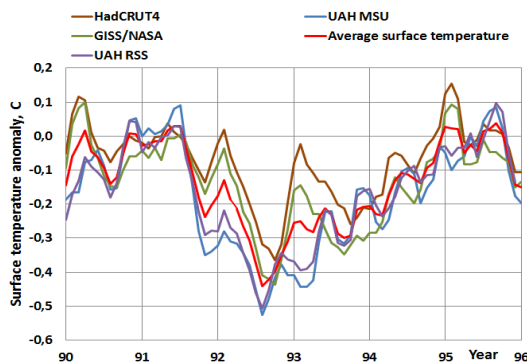


Fig. 8. Surface temperature anomalies according to four datasets

Because the quantified effects of ENSO are so controversial, this study has used the results of the own analyses. The elimination of ENSO is based on the analysis of ONI values (Oceanic Niño Index) [45] and the global ΔT values. The ENSO effect creates fluctuations, which can be identified as almost identical fluctuations of ΔT values after 1-12 months delay. The four most regular El Niño / La Niña cases were selected. The relationship from peak to peak between these fluctuations show that $\Delta T = 0.144 * \Delta \text{ONI}$ on average. This temperature effect formula has been used in modifying the measured ΔT values but there is no time delay applied, because the peak values of ONI and ΔT values match. In Fig. 9 is depicted the ENSO effect as a temperature anomaly and its effect on the two global ΔT trends. This approach gives the maximum ENSO effect of $\sim 0.23^{\circ}\text{C}$. The ENSO

during the Pinatubo eruption has a special feature not having the negative La Niña temperature peak at all.

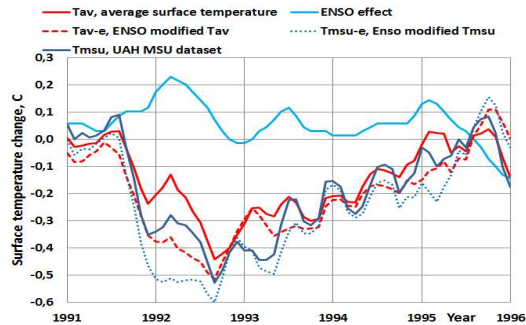


Fig. 9. The ENSO signal removed from the surface temperature measurement

The ENSO effect explains quite well why there is a peak upward from January 1992 to July 1992, when the surface temperature should be in minimum because of forcing by $\Delta \text{SWIN} / \Delta \text{LWDN}$ anomaly. After 1993 the ENSO effect is very small, but it caused an upward tick at the end of 1995, when the Pinatubo event was practically over. The ENSO modified surface temperatures Tav-e and Tmsu-e have been used as references in this study.

3. DYNAMIC MODEL SIMULATIONS

The Pinatubo eruption happened in such a way that the forcing factors in the form of ΔSWIN and ΔLWDN flux anomalies changed all the time and therefore the applied model must be dynamical. A dynamical model is capable of simulating time dependent variables and their impacts. In this case a simple dynamical model DM has been applied as described in Fig. 10.

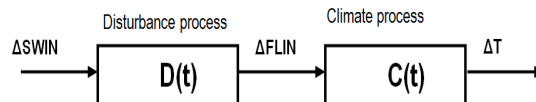


Fig. 10. The dynamic simulation model of the climate system

The output ΔFLIN of the disturbance process $D(t)$ is the difference of ΔSWIN and ΔLWDN created by the Pinatubo eruption. ΔFLIN has been delayed by 1.6 months called dead time in process dynamics and it can be formulated as follows:

$$\Delta FLIN = \Delta SWIN(t-t_D) - \Delta LWDN(t-t_D) \quad (2)$$

where t is time and t_D is dead time. The input variable $\Delta SWIN$ is a flux anomaly signal varying according to the time as depicted in Fig. 6. Also $\Delta LWDN$ varies according to the time as depicted in Fig. 7. The climate process $C(t)$ includes two elements: 1) the input signal $\Delta FLIN$ is transformed into the surface temperature change and 2) the dynamic behaviors of the climate system delays according two parallel first order transfer systems are included into ΔT effects:

$$\Delta T = \lambda * \Delta FLIN * (K_{sea} * \exp(-t/T_{sea}) + K_{land} * \exp(-t/T_{land})) \quad (3)$$

where t is time (months), \exp is exponent, K_{sea} is 0.7, K_{land} is 0.3, T_{sea} is a time constant of 2.74 months and T_{land} is a time constant of 1.04 months. These values are based on the earlier studies [12,46,47]. The values of the K parameters are the area portions of land and ocean of the Earth. The climate process $C(t)$ is a combination of two parallel processes, because the time delays of land and ocean are different.

Three different simulation cases have been described and carried out: 1) $\Delta SWIN$ and $\Delta LWUP$ (the proxy of the $LWDN$) fluxes are from ERBS datasets, 2) $\Delta SWIN$ and $\Delta LWDN$ are estimated as described above based on the AT measurements, 3) Feedback process experiment. The ISCCP dataset turned out to be too swaying and unreliable and therefore it has not been used. In cases 1) and 2) the simulations have been carried out by λ values of 0.27 $K/(Wm^{-2})$ and 0.5 $K/(Wm^{-2})$.

The dynamic processes according to eq. (2) are first-order dynamic models, which can be simulated in the discrete form enabling continuously changing input variables:

$$Out(n)=(\Delta t/(T+\Delta t))/((T/\Delta t)*(Out(n-1)+In(n)),(4)$$

where $Out(n)$ is the output of the process in step n , $In(n)$ is the input of the process of step n , T is the time constant, Δt is the simulation step interval ($=0.2$ months), and $n-1$ is the previous step value.

The results of using ERBS flux values are depicted in Fig. 11.

It can be noticed that the simulated temperature values vary a lot because the fluxes $\Delta SWIN$ and $\Delta LWIN$ vary too much. Especially the λ value of

0.5 $K/(Wm^{-2})$ gives ΔT_m peak values, which are almost double as large as the ΔT_m values using the λ value of 0.27 $K/(Wm^{-2})$. A possible reason for this is that the $LWUP$ flux anomaly is not an accurate enough estimate of the real $\Delta LWDN$ flux anomaly and the flux measurements are too inaccurate.

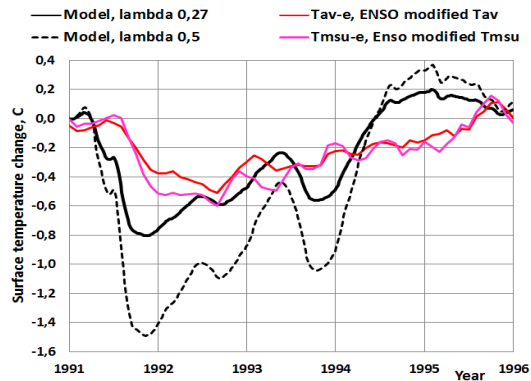


Fig. 11. The simulated surface temperature according to the dynamic DM using ERBS dataset $\Delta SWIN$ and $\Delta LWUP$ fluxes

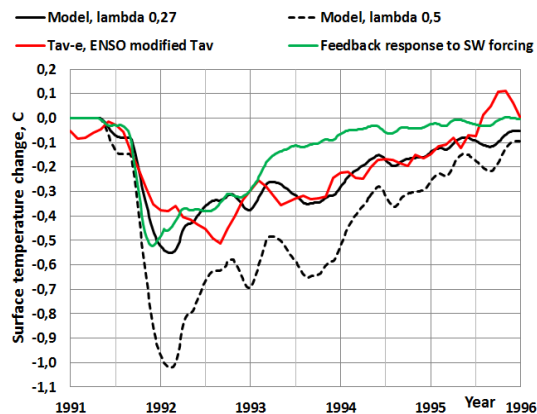


Fig. 12. The simulated surface temperature according to the dynamic model using estimated $SWIN$ and $LWDN$ fluxes

In Fig. 12 the same graphs are depicted, when the $\Delta SWIN$ and $\Delta LWDN$ are estimated according to the AT and aerosol optical depth measurements. The simulated ΔT_m signal is stable and the dynamic changes follow very well the real temperature changes ΔT . Also in this case the λ value of 0.5 $K/(Wm^{-2})$ gives results, which do not follow the real changes of the surface temperature changes but gives about 100% too great ΔT_m during the eruption.

The question of feedback has created the two schools of thoughts. Some researchers think that the climate system is like the other processes of the nature, which are built on negative feedbacks. A positive feedback system is dangerous, because it drives any system out of balance sooner or later. IPCC and some other researchers think that the climate system for example includes the positive water feedback as well as positive albedo and cloud feedbacks [17]. It should be noticed that the positive water feedback is included into the climate feedback parameter λ , when its value is $0.5 \text{ K}/(\text{Wm}^{-2})$ [16] and should results in a constant RH trend in the troposphere. The λ -value of $0.27 \text{ K}/(\text{Wm}^{-2})$ means a constant water content of the atmosphere.

A theoretical feedback process is simulated using the process model depicted in Fig. 13.

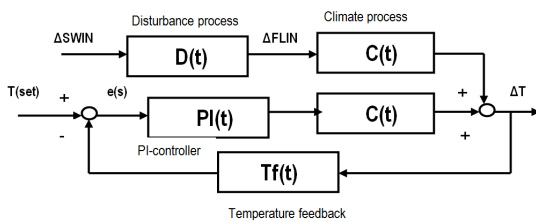


Fig. 13. A theoretical feedback process in the case of Pinatubo eruption

The theoretical feedback process can be constructed based on the assumption that the ΔSWIN flux anomaly is the only disturbance in a very stable climate system, which tries to eliminate this disturbance. The elimination process is a theoretical PI-controller, which detects a change in the surface temperature and creates an eliminating phenomenon, which tries to minimize the disturbance. In this case the eliminating flux is the ΔLWDN flux. The climate process $C(s)$ has as an input only the ΔSWIN anomaly. The PI-controller imitates the counter effect of ΔLWDN flux but ΔLWDN flux values are not needed to use in this simulation.

The mathematical form of the PI-controller (Proportional-Integral) in time domain is

$$\text{Out}(t) = K_p * e(t) + (1/T_i) * \int e(t) dt \quad (5)$$

Where K_p is the gain of the controller, T_i is the integral time and $e(t)$ is the error signal between the set point and the measurement. The equation (4) simulated in a discrete form in the time domain is

$$\text{Out}(t) = K_p * \Delta e(t) + (K_p/T_i) \sum e(t) \Delta t \quad (6)$$

The PI-controller was tuned by trial and error giving $K_p = 2$ and $T_i = 500$ months. The results of the negative feedback process simulation are depicted in Fig. 12. The output of the theoretical feedback process follows the ΔT_m values of DM surprisingly closely up to the end of 1993 as well as the measured ΔT values.

One big difference between this study and the three referred studies [32,35,36] is the use of estimated ΔLWDN instead of measured ΔLWUP fluxes. The basic reason is that these two fluxes have different values. The measured ΔLWUP fluxes are not stable, making the results very unstable too. This problem can be eliminated to a certain degree by heavy smoothing or even by removing parts of a flux signal [35].

The actual ΔLWUP flux depends on the surface temperature changes ΔT which is caused by the RF change. The RF is the sum of $\Delta\text{SWIN} + \Delta\text{LWDN}$ flux changes. The ΔLWUP flux can be calculated using the measured ΔT changes. The author has used two calculation methods. The first is MODTRAN radiation code available through Internet [18]. By applying the average global atmosphere profile, MODTRAN can calculate the LWUP flux change at TOA. The main parameters selected for these calculations were: CO_2 357 ppm, fixed water vapor pressure, cloudy sky with cumulus cloud base of 0.66 km and top of 2.7 km. The 1°C change in the surface temperature gives ΔLWUP change of 3.39 Wm^{-2} for the clear sky and 3.08 Wm^{-2} for the cloudy sky at TOA.

By combining the two sky conditions, the all-sky value of 3.18 can be calculated [10]. Ollila [10] has calculated the same relationship using another commercial spectral analysis tool Spectral Calculator for the clear sky conditions. The cloudy sky fluxes are estimated to be 25% less than the clear sky fluxes [16]. This calculation method gives the ΔLWUP change of 3.05 Wm^{-2} for the 1°C change. The results of MODTRAN calculation have been used, which gives a linear relationship

$$\Delta\text{LWUP} = 3.18 * \Delta T. \quad (7)$$

This linear relationship is applicable inside the small temperature change of 1°C .

The surface temperature calculated ΔLWUP is depicted in Fig. 14. It can be compared to the

measured Δ LWUP flux, which is in this case the average of ISCCP and ERBS datasets. The flux values are at about the same level except for the first months of 1992. The SW+LW forcing flux is about 1 Wm^{-2} higher than the ISCCP & ERBE flux during the period 3/1992 – 10/1992. This could be due to the error of LWDN flux estimate.

The LWDN flux may reduce quicker than the optical depth measurement indicates. This is also a probable reason for the difference between the T_m value of DM and the measurement based temperature anomalies during the year 1992. This is a very good result showing that Δ LWUP depends on Δ SWIN + Δ LWDN fluxes and their dynamic effects on the ΔT at the Earth's surface. Therefore, Δ LWUP is not really the right choice in calculating the surface temperature changes caused by downward radiation flux anomalies of SWIN and LWDN.

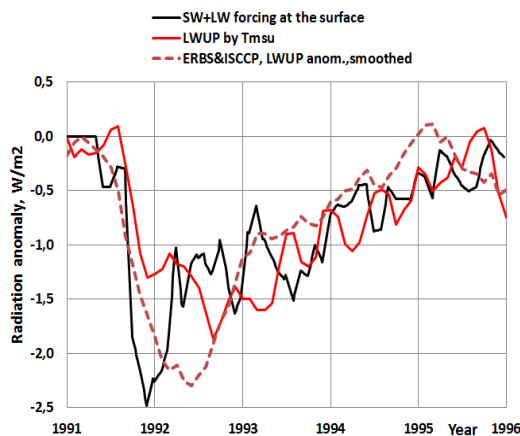


Fig. 14. The LW fluxes during the Pinatubo eruption

4. RESULTS AND DISCUSSION

These results can be compared to the results calculated by Hansen et al. [34] and Soden et al. [35] who have used complicated GCMs in their analyses. In these models the temperature effects are based on the eruption aerosol amounts and properties. When comparing the dynamic behavior, the calculated T_m of GCMs follows very accurately the real temperature change as does the DM. The conclusion is that the dynamical time delays in their GCMs must come very close to the time constants applied in this study.

The peak values of T_m of the GCM studies are -0.6°C [34] and -0.7°C [35] and according to their graphs, the model-predicted values are

practically same as the observed values. The observed values of this study vary from -0.5°C to -0.6°C based on the selected temperature measurement. One explanation could be that in the referred GCM studies the modified UAH MSU dataset has been used having a greater ENSO effect correction than in this study.

In the GCM calculations the researchers [34]-[35] have used ERBS flux values. In both cases the maximum value of SW anomaly Δ SWIN has been about -4 Wm^{-2} , which differs 33% from the value of -6 Wm^{-2} used in the majority of the other GCM studies and also in this study. The maximum LW anomaly Δ LWUP used in the GCM studies has been about -2.3 Wm^{-2} . Using equation (1) for steady-state conditions, the calculated peak T_m would be $0.5 * (-4 + 2.3) = -0.85^\circ\text{C}$. This value is very close to the model-predicted value of Soden et al. [35]. On the other hand, if the commonly used value of -6 Wm^{-2} would have been used, the calculated peak T_m would be $0.5 * (-6 + 2.3) = -1.85^\circ\text{C}$. If the average λ -value of $1.0 \text{ K}/(\text{Wm}^{-2})$ commonly found in GCMs is used, the T_m would be even larger. The GCM simulations of Soden et al. [35] gave results which are close to the measured ΔT values. The major features of these two studies are listed in Table 2.

The model calculated T_m values are for equilibrium conditions and the values of the real dynamic conditions are in brackets. The dynamic simulations of this study show that in the dynamic change condition the real equilibrium T_m value cannot be reached but the real temperature change is about $+0.1^\circ\text{C}$ smaller. The values in Table 2 show that the results of Soden et al. [35] can be generated using the λ value of $0.5 \text{ K}/(\text{Wm}^{-2})$ and the flux values applied by them.

This simple analysis shows that the model-predicted T_m values are completely dependent on the selected forcing fluxes, λ values and even on the selected observed ΔT value. It appears that in GCM simulations [34,35] the selected Δ SWIN flux cannot be regarded as the justifiable choice. Actually the greatest uncertainty is about the right Δ LWDN flux values, because there are no direct measurements available. The commonly used Δ LWUP flux at the TOA, is not the same flux as Δ LWDN. Δ LWUP is mainly dependent on the real RF fluxes (Δ SWIN and Δ LWDN) and on the surface temperature. Therefore the Δ LWUP flux contains the dynamic delays of the land and ocean and the

Table 2. Comparison of the major differences between the study of Soden et al. [35] and this study

	Soden et al.	Ollila
Min. Δ SWIN, Wm^{-2} , min.	-4.0	-6.0
Max. Δ LWDN, Wm^{-2} , max.	+2.3	+3.6
Max. radiative forcing, Wm^{-2}	-1.7	-2.4
Equil. Tm according to $\lambda = 0.5$ K/(Wm^{-2}), $^{\circ}C$	-0.85 (-0.75)	-1.2 (-1.1)
Equil. Tm according to $\lambda = 0.27$ K/(Wm^{-2}), $^{\circ}C$	-0.46 (-0.36)	-0.65 (-0.55)

warming/cooling effects of the forcing radiation fluxes. In the dynamic simulations this is a source of error. The real measured Δ LWUP fluxes are very spiky – especially ISCCP fluxes.

5. CONCLUSION

The results show that a simple one dimensional dynamic model DM gives results that are close to the real surface temperature changes ΔT after the Mount Pinatubo eruption using the climate sensitivity parameter value of 0.27 K/(Wm^{-2}). Timewise the changes follow very well the real changes. It means that the applied time constants for land (1.04 months) and for ocean (2.74 months) are accurate and can be used in any dynamic simulations. Especially the quick and large ΔT during the early phase of the eruption shows that the applied DM follows very accurately the real change rate.

The maximum temperature decrease differs $+0.05^{\circ}$ from the lowest dataset value (UAH MSU) and $-0.04^{\circ}C$ from the highest dataset value (T average) being actually in the middle of the dataset changes. This is a very good accuracy.

The climate sensitivity parameter value of 0.5 K/(Wm^{-2}) gives the minimum peak value of $-1.02^{\circ}C$, which is almost double in comparison to $-0.55^{\circ}C$ calculated by λ value of 0.27 K/(Wm^{-2}). This means that the climate models are very sensitive to the value of the climate sensitivity parameter. The mean λ -value of 1.0 K/(Wm^{-2}) commonly used in GCMs would give 200% too high values.

In this study Δ SWIN and Δ LWDN fluxes have also been estimated utilizing the apparent transmission measurements. The simulation using these fluxes gives the best and consistent results. The theoretical feedback simulation gives values which are close to the DM model values applying also the Δ LWDN flux values.

The correlation analysis between the model calculated Tm and the measured Tav-e gave the

correlation $r_2 = 0.6$ and the standard error of Tm = $0.066^{\circ}C$. When the standard error of Tm is transformed into the standard error of λ , the value is 0.036 K/(Wm^{-2}). This means that the uncertainty of λ is in the range from 0.234 K/(Wm^{-2}) to 0.306 K/(Wm^{-2}). The main reason for the relatively poor correlation seems to be the inaccurate surface temperature measurements. The correlation r_2 between Tmsu-e and Tav-s is 0.85 and the standard error of the estimate $0.040^{\circ}C$. This error is 61% of the standard error of the DM predicted temperature. If the 7 months running mean is applied to Tm and Tav-e like in the study of [35], $r_2 = 0.76$ and the uncertainty range of λ improves from 0.245 to 0.295 .

The theoretical simulation of negative feedback of the climate system gives Tm results, which follow well both the DM results and the real ΔT measurements.

COMPETING INTERESTS

Author has declared that no competing interests exist.

REFERENCES

1. Russel PB, Livingston JM, Pueschel RF, Bauman JJ, Pollack JB, Brooks SL, et al. Global to microscale evolution of the Pinatubo volcanic aerosol derived from diverse measurements and analyses. *Journal of Geophysical Research*. 1996;101:18745-18763.
2. Gu L, Baldocchi DD, Wofsy SC, Munger JW, Michalsky JJ, Urbanski SP, Boden TA. Response of a deciduous forest to the Mount Pinatubo eruption. *Science*. 2003; 299:2035-2038.
3. Farquhar GD, Roderick ML. Pinatubo, diffuse light and the carbon cycle. *Science*. 2003;299:1997-1998.
4. Stowe LL, Carey RM, Pellegrino PP. Monitoring the Mount Pinatubo aerosol layer with NOAA-11 AVHRR Data.

- Geophysical Research Letters. 1992;19:159-162.
5. UAH MSU temperature dataset. Available:<http://www.nsstc.uah.edu/data/msu/>
 6. Apparent transmission dataset at Mauna Loa. Available:http://www.esrl.noaa.gov/gmd/wesrdata/grad/mloapt/mlo_transmission.dat
 7. Wild M, Gilgen H, Roesch A, Ohmura A, Long CN, Dutton EG, et al. From dimming to brightening: Decadal changes in solar radiation at Earth's surface. *Science*. 2005;308:847-850.
 8. Thomas MA. Simulation of the climate impact of Mt. Pinatubo eruption using ECHAM5. Dissertation at Hamburg University; 2008.
 9. Minnis P, Harrison EF, Stowe LL, Gibson GG, Denn FM, Doelling DR, Smith WL. Radiative climate forcing by the Mount Pinatubo eruption. *Science*. 1993; 259:1411-1415.
 10. Raschke E, Kinne S, Stackhouse PW. GEWEX Radiative Flux Assessment (RFA). WCRP Report No. 19/2012; 2012.
 11. Ollila A. Earth's energy balance for clear, cloudy and all-sky conditions. *Development in Earth Science*. 2013;1.
 12. Ollila A. Dynamics between clear, cloudy and all-sky conditions: Cloud forcing effects. *Journal of Chemical, Biological and Physical Sciences*. 2013;4:557-575.
 13. Stenchikov GL, Kirchner I, Robock A, Graf HF, Antuna JC, Grainer RG, et al. Radiative forcing from the 1991 Mount Pinatubo volcanic eruption. *Journal of Geophysical Research*. 1998;103:13837-13857.
 14. Kirchner I, Stenchikov GL, Graf H-F, Robock A, Antuna JC. Climate model simulation of winter warming and summer cooling following the 1991 Mount Pinatubo volcanic eruption. *Journal of Geophysical Research*. 1999;104:19039-19055.
 15. Graf HF, Kirchner A, Robock A, Schyllt I. Pinatubo eruption winter climate effects. Model versus observations. *Climate Dynamics*. 1993;9:81-93.
 16. IPCC. Climate response to radiative forcing. IPCC Fourth Assessment Report (AR4), The physical science basis, contribution of working Group I to the fourth assessment report of the intergovernmental panel on climate change, Cambridge University Press, Cambridge; 2007.
 17. IPCC. The physical science basis. Working Group I contribution to the IPCC Fifth assessment report of the intergovernmental panel on climate change, Cambridge University Press, Cambridge. 2013.
 18. MODTRAN radiation code. Available:<http://climatemodels.uchicago.edu/modtran/>
 19. Ollila A. The potency of carbon dioxide (CO₂) as a greenhouse gas. *Development in Earth Science*. 2014;2:20-30.
 20. NOAA. Relative humidity trends. NOAA Earth System Research Laboratory. Available:<http://www.esrl.noaa.gov/gmd/aggl/>
 21. Held IM, Soden BJ. Water vapor feedback and global warming. *Annual Review of Energy and Environment*. 2000;25:441-475.
 22. Aldrin M, Holden M, Guttorp P, Bieltvedt Skeie R, Myhre G, Koren Berntsen GT. Bayesian estimation on climate sensitivity based on a simple climate model fitted to observations of hemispheric temperature and global ocean heat content. *Environmetrics*. 2012;23:253-271.
 23. Bengtson L, Schwartz SE. Determination of a lower bound on earth's climate sensitivity. *Tellus B*; 2012. Available:<http://dx.doi.org/10.3402/tellub.v65i0.21533>
 24. Lewis NJ. An objective bayesian improved approach for applying optimal fingerprint techniques to estimate climate sensitivity. *Journal of Climate*. 2013;26:7414-7429.
 25. Otto A, Otto FEL, Boucher O, Church J, Hegeri G, Piers M, et al. Energy budget constraints on climate response. *Nature Geoscience*. 2013;6:415-416. Available:<http://dx.doi.org/10.1038/ngeo1836>.
 26. Harde, H. Advanced two-layer climate model for the assessment of global warming by CO₂. *Open Journal of Atmospheric and Climate Change*. 2014;1:1-50.
 27. Lindzen RS, Yong-Sang C. On the observational determination of climate sensitivity and its implications. *Asia-Pacific Journal of Atmospheric Sciences*. 2011;47:377-390.
 28. Ramachandran S, Ramaswamy V, Stenchikov GL, Robock A. Radiative impact of the Mount Pinatubo volcanic eruption: Lower stratospheric response.

- Journal of Geophysical Research. 2000;105:409-424.
29. Yang F, Schlesinger ME. On the surface and atmospheric temperature changes following the 1991 Pinatubo volcanic eruption: A GCM study. Journal of Geophysical Research. 2002;107:4073.
 30. Forster F, Collins M. Quantifying the water vapour feedback associated with post-Pinatubo global cooling. Climate Dynamics. 2004;23:207-214.
 31. Kelly PM, Jones PD, Pengqun J. The spatial response of the climate system to explosive volcanic eruptions. International Journal of Climatology. 1996;16:537-550.
 32. Hansen J, Lacis A, Ruedy R, Sato M. Potential climate impact of Mount Pinatubo eruption. Geophysical Research Letters. 1992;19:215-218.
 33. Timmreck C, Graf H-F, Kirchner I. A one and a half year interactive MAECHAM4 simulation of Mount Pinatubo aerosol. Journal of Geophysical Research. 1999;104:9337-9359.
 34. Hansen J, Sato M, Ruedy R, Lacis A, Asamoah K, Borenstein S, et al. A Pinatubo climate modelling investigation. NATO ASI Series. 1996;l:233-272.
 35. Soden BJ, Wetherald RT, Stenchikov GL, Robock A. Global cooling after the eruption of Mount Pinatubo: A test of climate feedback by water vapor. Science. 2002;296:727-730.
 36. Vonder Haar TH, Bytheway JL, Fortsyth JM. Weather and climate analyses using improved global water vapor observations. Geophysical Research Letters. 2012;39:L16802. DOI:10.1029/2012GL052094
 37. NVAP dataset. NCEP/NCAR Reanalysis. Available:<http://www.esrl.noaa.gov/psd/data/timeseries/>
 38. ISCCP radiation fluxes. Available:<http://isccp.giss.nasa.gov/products/products.html>
 39. ERBS radiation fluxes. Available:https://eosweb.larc.nasa.gov/project/erbe/erbe_table
 40. HadCRUT4 temperature dataset. Available:https://eosweb.larc.nasa.gov/project/erbe/erbe_table
 41. GISS/NASA temperature dataset. Available:http://data.giss.nasa.gov/gistemp/tabledata_v3/GLB.Ts+dSST.txt
 42. UAH RSS temperature dataset. Available:http://data.remss.com/msu/monthly_time_series/RSS_Monthly_MSU_AMSU_Channel_TLT_Anomalies_Land_and_Ocean_v03_3.txt
 43. Santer BD, Wigley TML, Doutriaux C, Boyle JS, Hansen JE, Jones PD, et al. Accounting for the effects of volcanoes and ENSO in comparisons of modelled and observed temperature trends. Journal of Geophysical Research. 2001;106:28033-28059.
 44. Thompson DWJ, Wallace JM, Jones PD, Kennedy JJ. Identifying signatures of natural climate variability in time series of global-mean surface temperature: Methodology and insights. Journal of Climate. 2009;22:6120-6141.
 45. NOAA Oceanic Nina Index – ONI. Available:http://www.cpc.ncep.noaa.gov/products/analysis_monitoring/ensostuff/onsoyears_1971-2000_climo.shtml
 46. Stine AR, Huybers P, Fung IY. Changes in the phase of the annual cycle of surface temperature. Nature. 2009;457:435-441.
 47. Kauppinen J, Heinonen JT, Malmi PJ. Major Portions in climate change: Physical approach. International Review of Physics. 2011;5:260-270.

© 2016 Ollila; This is an Open Access article distributed under the terms of the Creative Commons Attribution License (<http://creativecommons.org/licenses/by/4.0>), which permits unrestricted use, distribution, and reproduction in any medium, provided the original work is properly cited.

Peer-review history:
 The peer review history for this paper can be accessed here:
<http://sciencedomain.org/review-history/13553>